Miner Deposita
DOI 10.1007/s00126-008-0183-5

LETTER

Anhydrite pseudomorphs and the origin of stratiform Cu–Co ores in the Katangan Copperbelt (Democratic Republic of Congo)

Ph. Muchez · P. Vanderhaeghen · H. El Desouky · J. Schneider · A. Boyce · S. Dewaele · J. Cailteux

Received: 14 September 2007 / Accepted: 5 March 2008
© Springer-Verlag 2008

Abstract The stratiform Cu–Co ore mineralisation in the Katangan Copperbelt consists of dispersed sulphides and sulphides in nodules and lenses, which are often pseudomorphs after evaporites. Two types of pseudomorphs can be distinguished in the nodules and lenses. In type 1 examples, dolomite precipitated first and was subsequently replaced by Cu–Co sulphides and authigenic quartz, whereas in type 2 examples, authigenic quartz and Cu–Co sulphides precipitated prior to dolomite and are coarse-grained. The sulphur isotopic composition of the copper–cobalt sulphides in the type 1 pseudomorphs is between −10.3 and 3.1‰ relative to the Vienna Canyon Diablo Troilite, indicating that the sulphide component was derived from bacterial sulphate reduction (BSR). The generation of HCO_3^- during this process caused the precipitation and replacement of anhydrite by dolomite. A second product of BSR is the generation of H_2S, resulting in the precipitation of Cu–Co sulphides from the mineralising fluids. Initial sulphide precipitation occurred along the rim of the pseudomorphs and continued towards the core. Precipitation of authigenic quartz was most likely induced by a pH decrease during sulphide precipitation. Fluid inclusion data from quartz indicate the presence of a high-salinity (8–18 eq. wt.% NaCl) fluid, possibly derived from evaporated seawater which migrated through the deep subsurface. $^{87}Sr/^{86}Sr$ ratios of dolomite in type 1 nodules range between 0.71012 and 0.73576, significantly more radiogenic than the strontium isotopic composition of Neoproterozoic marine carbonates ($^{87}Sr/^{86}Sr$=0.7056–0.7087). This suggests intense interaction with siliciclastic sedimentary rocks and/or the granitic basement. The low carbon isotopic composition of the dolomite in the pseudomorphs (−7.02 and −9.93‰ relative to the Vienna Pee Dee Belemnite, V-PDB) compared to the host rock dolomite (−4.90 and +1.31‰ V-PDB) resulted from the oxidation of organic matter during BSR.

Keywords Anhydrite · Copperbelt · Cu–Co stratiform ore deposits · Fluid chemistry · Bacterial sulphate reduction · Democratic Republic of Congo

Editorial handling: R. Moritz

Ph. Muchez (✉) · P. Vanderhaeghen · H. El Desouky · J. Schneider
Geodynamics & Geofluids Research Group, Afdeling Geologie,
K.U.Leuven,
Celestijnenlaan 200E,
3001 Leuven, Belgium
e-mail: philippe.muchez@geo.kuleuven.be

J. Schneider
Centre for Archaeological Sciences, K.U.Leuven,
Celestijnenlaan 200E,
3001 Leuven, Belgium

A. Boyce
Isotope Geoscience Unit, SUERC,
Rankine Avenue, East Kilbride,
Glasgow G75 0QF, UK

S. Dewaele
Department of Geology and Mineralogy,
Royal Museum for Central Africa (RMCA),
Leuvensesteenweg 13,
3080 Tervuren, Belgium

J. Cailteux
Département Recherche et Développement, EGMF,
Groupe G. Forrest International,
Lubumbashi, Democratic Republic of Congo

Introduction

The Central African Copperbelt hosts stratiform Cu–Co deposits of major economic importance within the lower

part of the Neoproterozoic Katanga Supergroup in the Democratic Republic of Congo (DRC) and Zambia (Fig. 1). The most widely proposed genetic model for these deposits favours a diagenetic ore formation (Bartholomé et al. 1972; Bartholomé 1974; Brown and Chartrand 1983; Cailteux et al. 2005; Brown 2005). However, recent investigations indicate that this model is not generally applicable to all stratiform deposits in the Central African Copperbelt (Hitzman et al. 2005; Selley et al. 2005). For instance, McGowan et al. (2006) presented field and isotopic evidence which suggests that the Nchanga deposit in Zambia is related to early inversion of the Zambian basin. In addition, the stratiform Cu–Ag mineralisation at Lufukwe, north of the Copperbelt, most likely formed after the late Neoproterozoic–early Palaeozoic Lufilian orogeny (El Desouky et al. 2007a). Stratiform Cu–Co mineralisation in both Zambia and the DRC consists of anhydrite nodules, lenses and layers which are replaced by carbonate, quartz and sulphide minerals (Annels 1974; Sweeney and Binda 1989). Evidence for the replacement of anhydrite by sulphides has been found, e.g. at Musoshi, Kamoto, Kambove and Luiswishi in the DRC (Cailteux 1997; Lerouge et al. 2005; El Desouky et al. 2007b) and at Konkola and Nkana in the Zambian part of the Copperbelt (Annels 1974; Sweeney et al. 1986). The anhydrite nodules are a characteristic feature of the evaporitic sedimentation environment of the mineralised Musoshi (Zambia) and Mines Subgroups (DRC, Cailteux et al. 2005). Based on a stable isotopic study, Sweeney et al. (1986) and Lerouge et al. (2005) concluded that the disseminated sulphides and the sulphides in the nodules and lenses formed by bacterial reduction of seawater sulphate during early diagenesis and suggested a link between sulphide and carbonate formation.

The aim of this study is to better understand the processes which led to the replacement of anhydrite by carbonate, quartz and Cu–Co sulphides in the Katangan part of the Central African Copperbelt. Mineralised Roan rocks from selected boreholes at Kamoto, Musonoi and Luiswishi (Fig. 1) were characterised by transmitted and reflected light microscopy and cathodoluminescence imaging. Stable and radiogenic isotopes (S–C–O–Sr) were used to constrain the source of the mineralising fluids and the conditions of ore formation.

Geology and mineralisation

The Neoproterozoic Katanga Supergroup comprises a >9-km-thick sedimentary succession in the Pan-African Lufilian Arc (Fig. 1) composed of alternating dolomites, dolomitic shales, siltstones, sandstones and arkoses. The Katanga Supergroup (Fig. 2) has been subdivided into the Roan, Nguba and Kundelungu Groups (Cailteux et al. 2005). Sedimentation of the Lower Katangan Roan Group commenced subsequently to intrusion, uplift and erosion of the Nchanga granite at ca. 880–870 Ma (Armstrong et al. 2005). For the overlying Nguba Group, U–Pb sensitive high-resolution ion microprobe dating of zircons from intercalated volcanic rocks yielded a maximum age of ca. 760 Ma (Key et al. 2001; Master et al. 2005). The Nguba Group spans approximately the period 760–620 Ma (Master et al. 2005). Both the Nguba and Kundelungu Groups contain diamictite horizons at their

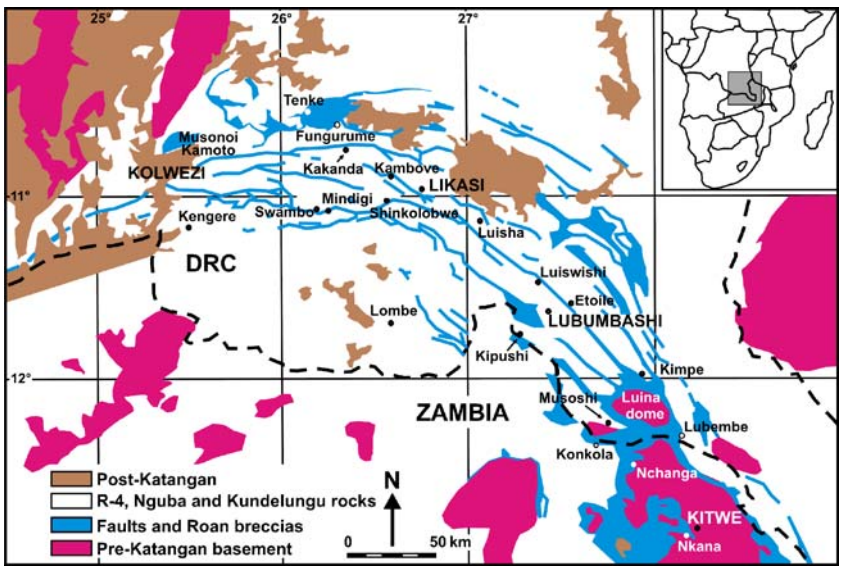

Fig. 1 Map of the Central African Copperbelt with the location of the deposits at Kamoto, Musonoi and Luiswishi (modified after François 1974)

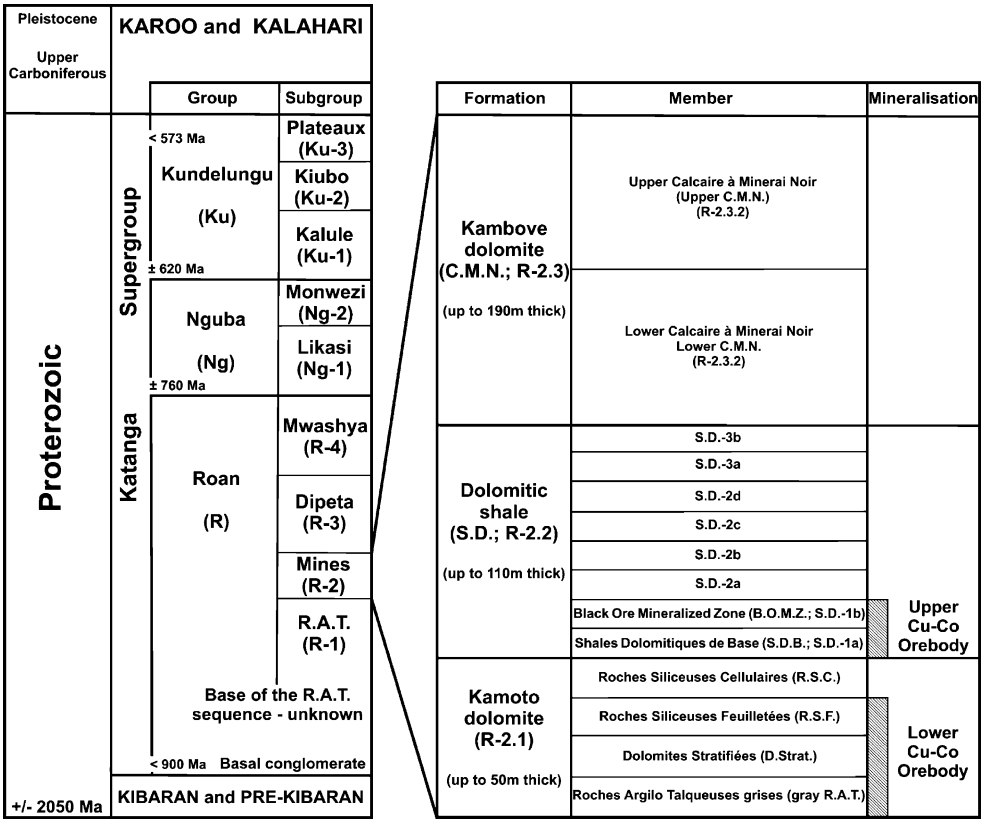

Fig. 2 Stratigraphy of the Katangan Supergroup in the Democratic Republic of Congo (modified after Cailteux et al. 2005)

base, which can be broadly correlated with other Neoproterozoic glacial deposits, e.g. in the Otavi Mountainland, northwestern Namibia (Cailteux and Kampunzu 2003; Batumike et al. 2007; Cailteux et al. 2007).

The mineralised Roan Group comprises siliciclastic and carbonate rocks (Cailteux et al. 1994) as well as volcanic and plutonic igneous rocks that were emplaced in a continental rift setting (Kampunzu et al. 2000; Cailteux et al. 2007). The Roan Group is subdivided into four subgroups: the Roches Argilo-Talqueuses (R.A.T., R-1), Mines (R-2), Dipeta (R-3) and the Mwashya (R-4) Subgroups (Fig. 2). The R-1 Subgroup consists of chlorite-rich dolomitic sandstones. The Mines Subgroup (R-2) is subdivided into three formations: the Kamoto dolomite (R-2.1), the Dolomitic shale (R-2.2) and the Kambove dolomite (R-2.3). The Dipeta Subgroup (R-3) is characterised by alternating dolomites and argillaceous dolomitic sandstones. The uppermost part of the Roan (R-4) consists of dolomitic or carbonaceous shales and silicified dolomites of the Mwashya Subgroup. The R.A.T., Mines and the Dipeta Subgroups formed in a marine evaporitic environment (Cailteux 1978a, b; Lefebvre 1989; Okitaudji 1992). The organic-rich shales and siltstones of the Mines Subgroup reflect reducing conditions (Cailteux et al. 2005). The Katanga basin closed during the Lufilian orogeny, which produced predominantly north-trending folds, thrusts and nappes (Daly et al. 1984; Kampunzu and Cailteux 1999).

The stratiform Cu–Co mineralisation extends from Kolwezi up to Kimpe in the DRC (Fig. 1). The Cu–Co ores occur at two main levels in the Mines Subgroup (R-2), namely at the bases of the Kamoto dolomite (R-2.1, lower orebody) and the Dolomitic shales (R-2.2, upper orebody; Figs. 2 and 3). The host rocks of the lower orebody consist of dolomitic siltstones, fine-grained dolomites and silicified stromatolitic dolomites alternating with chloritic, dolomitic siltstones, while the host rocks to the upper orebody include dolomitic shales and coarse-grained dolomites (Cailteux 1994; Cailteux et al. 2005). Although the deposits are typically interpreted to be stratiform (Fig. 4a,b and c), this definition applies only partly to the mineralisation as many deposits display multiple vein generations (Annels 1989; Cailteux et al. 2005; Dewaele et al. 2006) that crosscut the stratification (Fig. 4d). The stratiform Cu–Co mineralisation in the DRC mostly consists of dispersed sulphides in the fine-grained rocks and in nodules, lenses and layers (for review see Cailteux et al. 2005).

The stratiform ore deposits at Kamoto, Musonoi and Luiswishi are interpreted as early diagenetic mineralisations (Bartholomé et al. 1972; Bartholomé 1974; Lerouge et al. 2005). Although disseminated sulphides and sulphides in nodules, lenses and layers form the dominant mineralisation

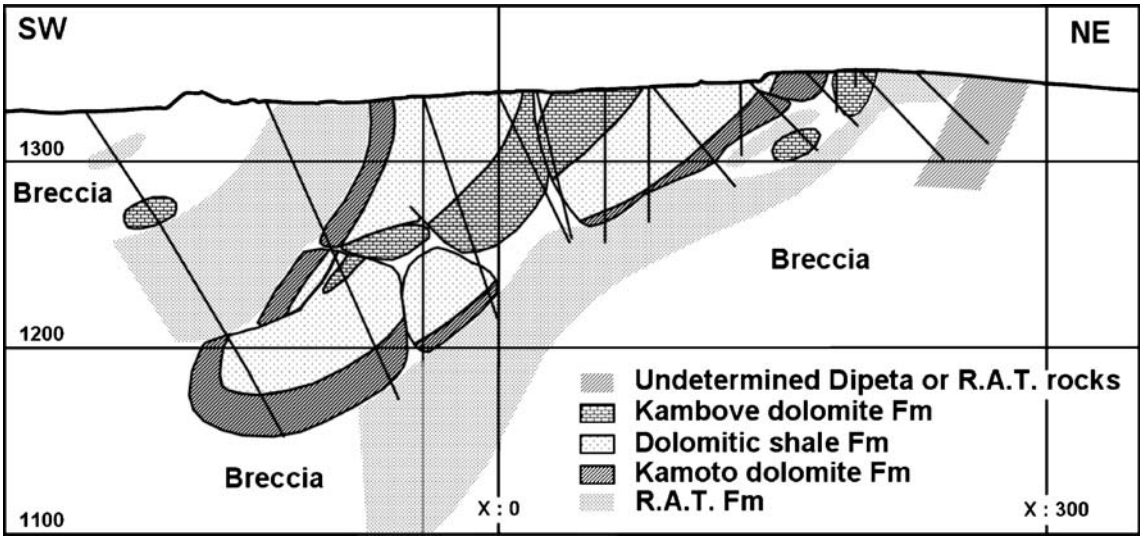

Fig. 3 Cross section through the Luiswishi ore deposit (after Cailteux et al. 2003). The lower orebody at Luiswishi occurs in the lower part of the Kamoto dolomite and the upper orebody at the base of the Dolomitic shale

type in the three deposits investigated, later mineralisation events and/or remobilisation are evident (Dewaele et al. 2006) which are significantly more important at Luiswishi than at Kamoto (El Desouky et al. 2007b). At Kamoto and Luiswishi, sulphides also occur in veins and as a cement in tectonic breccias (Fig. 4d and e) (Lerouge et al. 2005; El Desouky et al. 2007b).

Production figures and total reserves of the mines are based on the extensive archive of the Royal Museum of Central Africa (Mineral occurrences database compiled by the RMCA, Tervuren, Belgium and GF Consult). Kamoto Principal open pit, Kamoto Principal underground mine, Kamoto North, Kamoto East and Kamoto–Oliveira–Virgule or KOV mine are the five mines at Kamoto. No data regarding past production at Kamoto are available; however, reserves are estimated at 50 Mt grading 4.4% copper and 0.5% cobalt. Exploitation of the oxidation zone at the Musonoi Principal open pit started in the 1940s. Data on past production are not available, except that by 1974 about 25 Mt of ore were estimated to have been extracted. In 1974, the reserves were estimated at ~25 Mt at 3.9–5.4% copper and 0.4–0.6% Co. The Luiswishi deposit was mined episodically for Cu and Co between 1929 and 1956 by the Union Minière du Haute Katanga. Open pit mining started again in 1998 by the Forrest Group in partnership with GECAMINES. Total resources were estimated at 8 Mt at 2.5% copper and 1.1% cobalt.

Methods

Thin and polished sections of rock samples of the Mines Subgroup were studied by transmitted and incident light and cathodoluminescence microscopy. Oxygen and carbon isotope analyses were completed at the University of Erlangen, Germany. The dolomite powders were reacted with 100% phosphoric acid (density >1.9; Wachter and Hayes 1985) at 75°C using a Kiel III online carbonate preparation line connected to a Thermo Finnigan 252 mass spectrometer. All values are reported in per mil relative to the Vienna Pee Dee Belemnite (V-PDB) by assigning a $\delta^{13}C$ value of +1.95 and a $\delta^{18}O$ value of −2.20 to NBS 19. Reproducibility was constrained by replicate analysis of laboratory standards and is better than ±0.04 (1σ) for both carbon and oxygen isotope ratios.

Rb–Sr isotopic data were produced for 12 dolomite samples. These were weighed, spiked with a mixed ^{84}Sr–^{87}Rb tracer and dissolved in 6 N HCl on a hot plate. After evaporation to dryness, the residues were redissolved in 3 N HNO_3. Rb and Sr were chemically separated with 3 N HNO_3 using EICHROM Sr resin on 50 µl Teflon columns, following the methods of Deniel and Pin (2001). The first HNO_3 wash (600 µl) containing the Rb fraction was evaporated to dryness, rewetted with 100 µl 6 N HCl and dried again. Sr was stripped from the columns with 1 ml of H_2O. For mass spectrometry, Sr was loaded with $TaCl_5$–HF–H_3PO_4 solution (Birck 1986) onto W single filaments. Rb was loaded with H_2O onto the evaporation ribbon of a Ta double-filament assemblage. All isotopic measurements were performed on a Finnigan MAT 262 solid-source mass spectrometer running in static multi-collection mode. Sr isotopic ratios were normalised to $^{86}Sr/^{88}Sr=0.1194$. Repeated static measurements of the NBS 987 standard over the duration of this study yielded an average $^{87}Sr/^{86}Sr$ ratio of 0.71024±3 (2σ mean, $n=5$). Total procedure blanks ($n=2$) amounted to 30 pg Sr and 4 pg Rb and were found to be negligible.

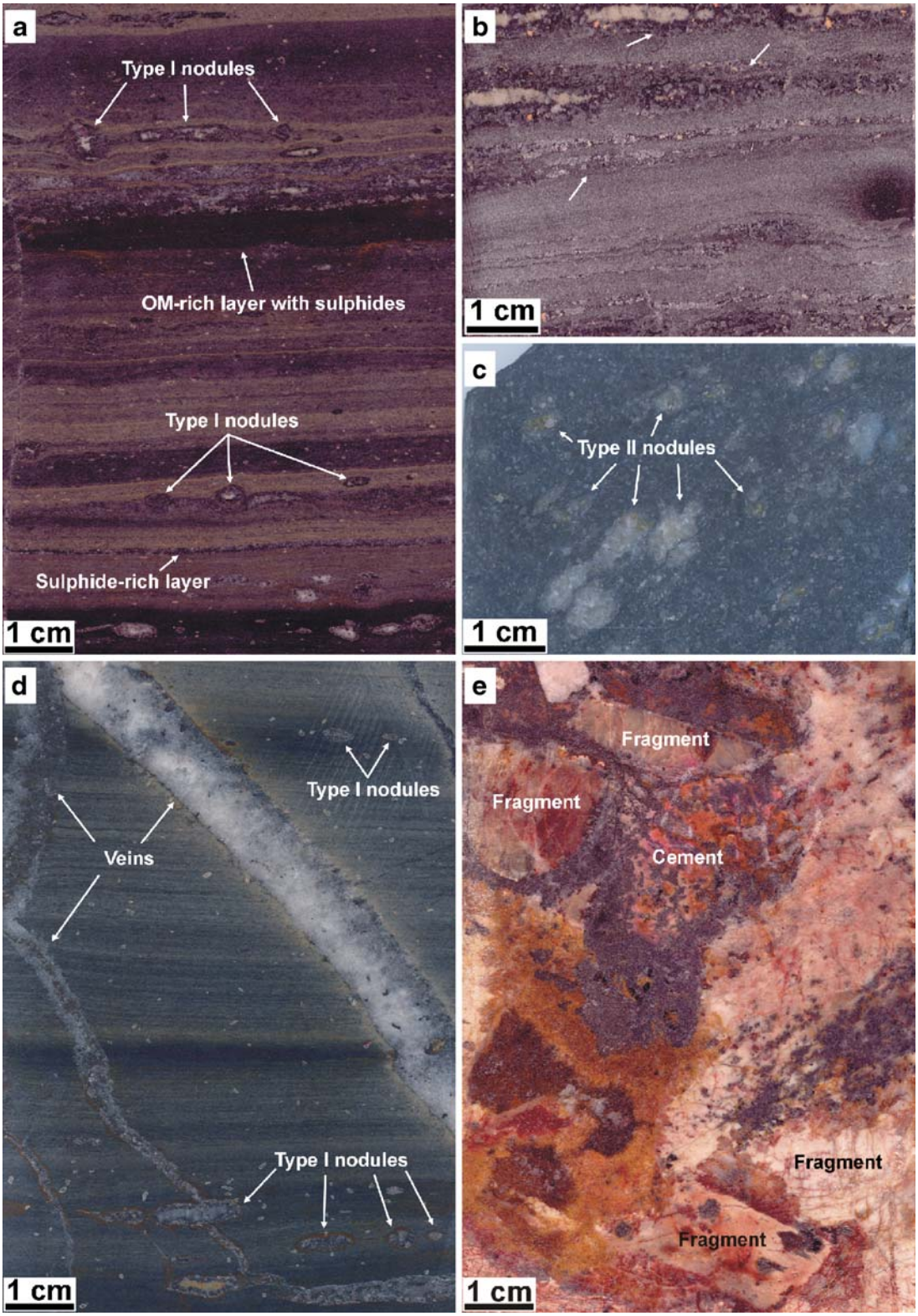

Fig. 4 **a** Type 1 nodules and sulphide-rich layers hosted in finely laminated siltstone and shale. "Shales dolomitiques de base" member (SDB), upper orebody Kamoto. **b** Sulphide-rich layers (*arrows*) in finely laminated dolomitic siltstone and shale. *OM* organic matter. "Roches siliceuses feuilletées" member (RSF), lower orebody Kamoto. **c** Type 2 nodules in fine-grained dolomite. Black ore mineralised zone member (BOMZ), upper orebody Luiswishi. **d**. Millimetre- to centimetre-thick veins in laminated dolomitic siltstone and shale. Vein crosscuts type 1 nodule in the lower part of the photograph. "Shales dolomitiques de base" member (SDB), upper orebody at Kamoto. **e** Breccia with fragments from the "Roches siliceuses cellulaires" member (RSC, Kamoto) cemented by dolomite, quartz and Cu–Co sulphides

The sulphur isotopic composition of the samples was analysed by in situ laser combustion from standard polished sections. An area of 300–400-μm diameters of the sulphide minerals was combusted using a Spectron Lasers 902Q CW Nd:YAG laser, in the presence of excess oxygen (Fallick et al. 1992). The released SO_2 gas was purified in a vacuum line, which operates similar to a conventional sulphur extraction line (Kelley and Fallick 1990). The sulphur isotopic composition of the purified SO_2 gas was measured using a VG SIRA II gas mass spectrometer. Sulphur isotope compositions are reported in standard per mil (‰) relative to the Canyon Diablo Troilite (V-CDT). The analytical precision, based on replicate measurements of international standards NBS-123 and IAEA-S-3 as well as an internal lab standard CP-1 (Scottish Universities Environmental Research Centre), was ±0.2‰.

Results

Petrography and fluid inclusion characteristics

Host rock

Pseudomorphs after evaporites occur in dolomite and dolomitic siltstone of the Mines Subgroup in the Katangan Copperbelt (Cailteux 1978a, b, 1994; Lefebvre 1978). The host rock comprises fine-grained xenotopic (sensu Friedman 1965) dolomite (micrometre-size crystals) or coarser-grained hypidiotopic dolomite (20–300 μm), which are both brown luminescent. Dispersed, framboidal pyrite occurs in the fine-grained rocks, reflecting the activity of sulphate-reducing bacteria in anaerobic sediments (Machel 2001); a reaction which occurs at temperatures below 80°C (Machel and Foght 2000). The framboidal pyrite is replaced and overgrown by chalcopyrite (see also Bartholomé et al. 1972; Brown and Chartrand 1983). Disseminated carrolite, bornite and chalcocite are associated with chalcopyrite. The crystal size of these sulphides varies between 20 and 150 μm, similar to the size of the framboidal pyrite. In addition, lenses of Cu–Co sulphides may reach one to several millimetres in thickness (Fig. 4a and b). Locally, the fine-grained dolomite recrystallised to a bright yellow luminescent dolomite, which also occurs as a cement postdating the opaque minerals in large cavities (up to several hundreds of micrometres) that form a porous network. The mineralised rocks are characterised by the precipitation of authigenic quartz associated with the mineralisation (Dewaele et al. 2006). The quartz has a composite texture and undulous extinction to the point that it is no longer clear where one crystal ends and another grain begins. The authigenic quartz may occur as individual growth, in clusters or massive and may replace completely the original laminated dolomitic siltstone. Detrital quartz and dolomite are absent in the silicified rock. However, randomly oriented muscovite is still preserved (Fig. 5a). Muscovite in this authigenic quartz is randomly oriented and may surround the sulphides in a rectangular way. Chalcopyrite that occurs disseminated in the laminated rock can also occur concentrated along the reaction front of authigenic quartz. Pyrite occurs both in the laminated host rock and the silicified samples, but the grain size is much larger in the silicified samples. This suggests remobilisation of sulphides during the formation of authigenic quartz. Dissolution of detrital quartz may also be restricted to coarse-grained layers, which is reflected in the presence of coarse-grained muscovite and the precipitation of authigenic quartz in clusters (Fig. 5a).

Pseudomorphs after anhydrite

Pseudomorphs after anhydrite are abundant in the Mines Subgroup (e.g. Cailteux 1978a, b, 1994; Lefebvre 1978). They occur in oval, round and cauliflower-shaped nodules, in lenses that may be wedge-shaped and as laths. Two main types of replacement and cementation of these structures can be distinguished. In type 1 (Fig. 4a), dolomite precipitated first and was replaced by Cu–Co sulphides and authigenic quartz. Relicts of anhydrite and halite are still present in these type 1 nodules and lenses (Fig. 6). In type 2 (Fig. 4c), the authigenic quartz and sulphides precipitated prior to dolomite and the crystals are coarse-grained and free-growing. Primary fluid inclusions in type 1 authigenic quartz belong to the H_2O–NaCl system, have a salinity between 8.4 and 18.4 eq. wt.% NaCl and homogenisation temperatures between 80 and 192°C (Dewaele et al. 2006). Primary fluid inclusions in type 2 authigenic quartz contain high-salinity (38.6 to 46.5 eq. wt. % NaCl) fluid inclusions with homogenisation temperatures between 324 and 419°C (El Desouky et al. 2007b). The characteristics of the fluid that caused replacement of the type 2 nodules and lenses by authigenic quartz are similar to the fluid inclusions present in quartz cement in late veins and a tectonic breccia (El Desouky et al. 2007b). This fluid reflects the mineralising conditions during deep burial and orogenesis and forms the topic of a separate study. The present study focuses on the characteristics and formation conditions of the type 1 nodules and lenses to obtain a better understanding of the processes that occurred during diagenesis.

Oval to rounded nodules vary in size between a few hundred micrometres and 5 mm. The nodules consist of a rim of authigenic quartz and sulphides such as chalcopyrite, bornite, carrolite and chalcocite. The size of the authigenic quartz crystals varies between 20 and 200 μm. The core of the nodules is composed of a brown luminescent hypidio-

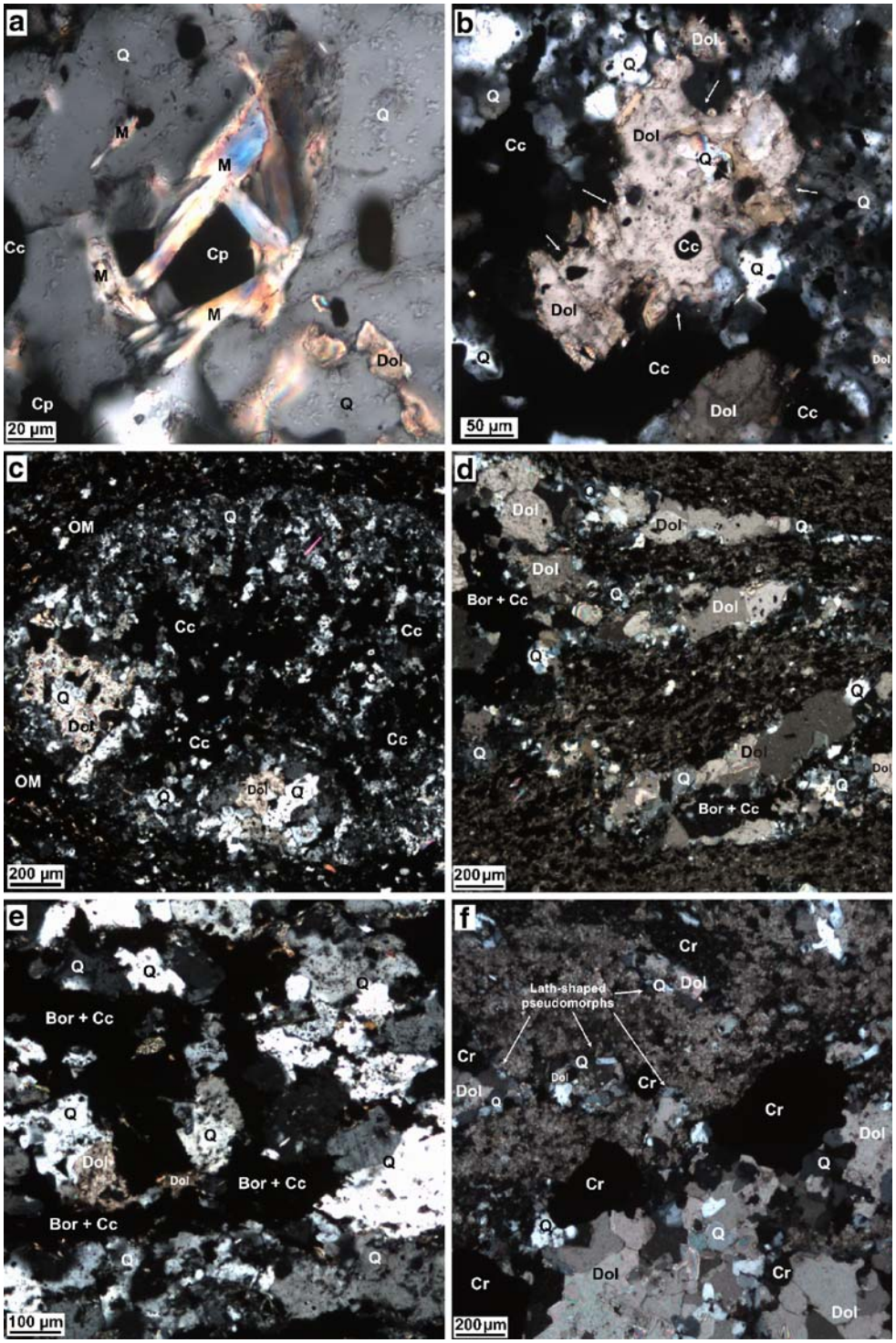

Fig. 5 **a** Muscovite (*M*) surrounds in a rectangular way chalcopyrite and is enclosed in massive authigenic quartz (*Q*). *Cp* chalcopyrite, *Cc* chalcocite, *Dol* dolomite; double-polarised light. **b** Pseudomorphic nodule after anhydrite consisting at its rim of authigenic quartz (*Q*) and chalcocite (*Cc*). Both minerals replace (*arrows*) dolomite (*Dol*) which is still present in the core of the nodule; double-polarised light. **c** Oval pseudomorph after anhydrite consisting of authigenic quartz (*Q*) and chalcocite (*Cc*) with relict dolomite crystals (*Dol*) in an organic-rich layer; double-polarised light. **d** Wedge-shaped pseudomorphs in dolomitic siltstone consisting of dolomite (*Dol*), authigenic quartz (*Q*) and bornite (*Bor*) and chalcocite (*Cc*); double-polarised light. **e** Pseudomorphic lens with authigenic quartz (*A*), bornite (*Bor*), chalcocite (*Cc*) and dolomite (*Dol*). Chalcocite occurs in authigenic quartz (*arrows*) but may also overgrow it; double-polarised light. **f** Lath-shaped pseudomorphs (*arrows*) composed of dolomite (*Dol*) and authigenic quartz (*Q*) and a part of a large cauliflower nodule consisting of authigenic quartz (*Q*), carrolite (*Cr*) and dolomite (*Dol*); double-polarised light

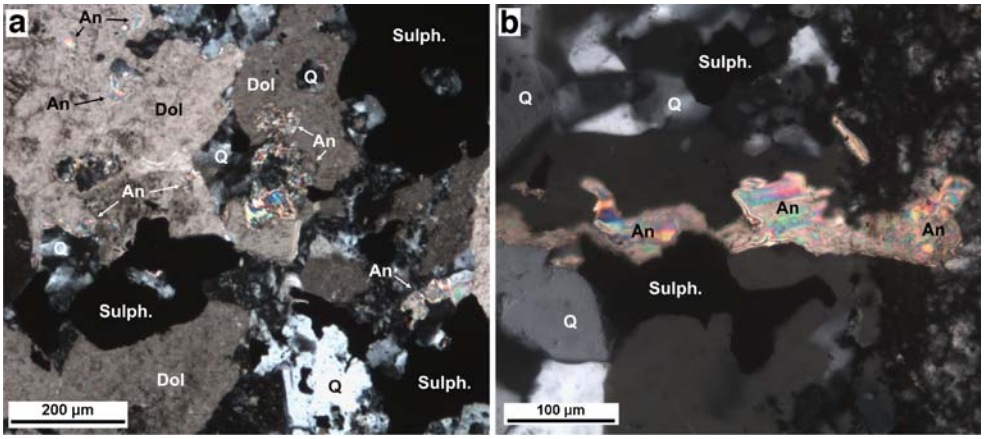

Fig. 6 Microphotographs of relicts of anhydrite in type 1 nodules. **a** Anhydrite relicts (*An*) hosted in and replaced by dolomite (*Dol*) in a large type 1 nodule also consisting of quartz (*Q*) and sulphides (*Sulph*), upper orebody at Kamoto. **b** Anhydrite relict (*An*) replaced by quartz (*Q*) and Cu–Co sulphides (*Sulph*) at the border of type 1 nodule, lower orebody at Kamoto

topic (sensu Friedman 1965) dolomite (up to 1.2 mm). Authigenic quartz and Cu–Co sulphides replace dolomite crystals (Fig. 5b) and therefore postdate dolomite formation. Although sulphides and authigenic quartz predominantly occur around the rim of the nodules and the dolomite in the core, the nodules may also be completely replaced by authigenic quartz and sulphides with a few relics of dolomite (Fig. 5c). Cauliflower nodules with a size up to 2 cm consist of a coarse-grained hypidiotopic dolomite (80–300 µm) with a zoned brown luminescence, authigenic quartz and Cu–Co sulphides. Organic matter occurs concentrated around the nodules (Fig. 5c).

Pseudomorphs after anhydrite are also found as lenses (size ranging between 250 µm to 1 mm width and 1.5 mm to 2.5 cm length). Wedge-shaped lenses are several centimetres long and up to 15 mm thick (Fig. 5d). The lenses are composed of authigenic quartz, bornite, carrolite, chalcopyrite, chalcocite and some relics of brown luminescent dolomite, which is replaced by authigenic quartz and sulphides. Quartz often contains inclusions of Cu–Co sulphides (Fig. 5e), but may also be overgrown by sulphides. Lath-shaped pseudomorphs after anhydrite (Fig. 5f) are ~400×100 µm in size and are composed of dolomite, authigenic quartz and sulphides. Carrolite is typically common in the pseudomorphs after anhydrite and therefore more abundant in rocks bearing these pseudomorphs, suggesting a genetic relationship.

Geochemistry

The sulphur isotopic composition of chalcocite, bornite and carrolite from type 1 nodules and lenses varies between −10.3 and +3.1‰ V-CDT (Fig. 7). The $\delta^{34}S$ values of disseminated and bedding-parallel chalcopyrite and carrolite at Luiswishi show a slightly larger range between −14.2 and +5.8‰ V-CDT (Lerouge et al. 2005).

The carbon and oxygen isotopic composition of the fine-grained dolomitic host rock and dolomite in the pseudomorphs is shown in Fig. 8. The $\delta^{18}O$ and $\delta^{13}C$ values of the host dolomite vary between −7.89 and −10.32‰ V-PDB and between −4.90 and +1.31‰ V-PDB, respectively (Fig. 8). The dolomite in the nodules has $\delta^{18}O$ values between −9.79 and −11.50‰ V-PDB, and $\delta^{13}C$ varies between −7.02 and −9.93‰ V-PDB (Fig. 8). The isotopic composition of Late Neoproterozoic marine dolomites ranges between −8 and −4‰ for oxygen and between −4.0 and +4.0‰ for carbon (Veizer and Hoefs 1976; Lindsay et al. 2005). Whilst the carbon isotopic composition of the host dolomite is compatible with Neoproterozoic marine carbonate carbon, $\delta^{18}O$ is shifted towards more negative values. The composition of the dolomite pseudomorphs falls outside this range and lies at the lower end of the range of the host rock dolomite.

The strontium isotopic composition of dolomite in the nodules shows a wide range with $^{87}Sr/^{86}Sr$ values up to 0.73576 (Table 1), but most values are between 0.71012 and 0.71332. These values are significantly more radiogenic than the strontium isotopic composition of Neoproterozoic marine carbonates, which range between 0.7056 and 0.7087 (Jacobsen and Kaufman 1999). There is no correlation between $^{87}Sr/^{86}Sr$ ratios and Sr elemental content (ca. 7–42 ppm) of the dolomite samples in a Sr mixing diagram (Fig. 9). Rb contents and $^{87}Rb/^{86}Sr$ ratios were determined for seven samples that either have low Sr concentration levels or radiogenic $^{87}Sr/^{86}Sr$ ratios (Table 1). These are generally very low, comparable to values presented by Allsopp and Ferguson (1970) for dolomite and vein calcite related to the Tsumeb mineralisation in the Otavi Mountainland, Namibia. $^{87}Rb/^{86}Sr$ and $^{87}Sr/^{86}Sr$ ratios are not correlated, indicating that in situ decay of ^{87}Rb is negligible with respect to the Sr isotopic composition of the Kamoto dolomite samples. Consequently, corrections performed even for an age of 800 Ma (Roan Group between <880 and 760 Ma) to determine "initial" Sr isotopic compositions have only insignificant effects on their $^{87}Sr/^{86}Sr$ ratios (Fig. 9).

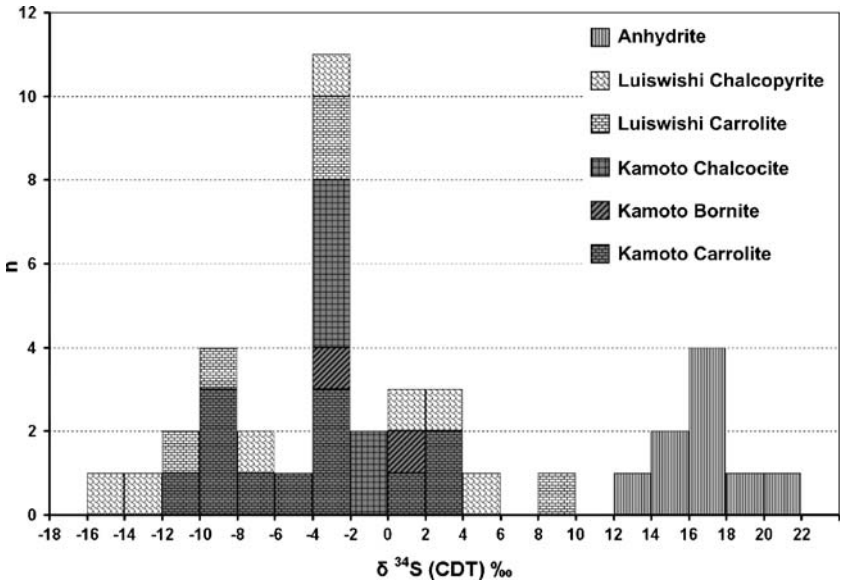

Fig. 7 Histogram of the sulphur isotopic composition of metal sulphides in the evaporite pseudomorphs in the ore bodies at Kamoto. The sulphur isotope data of disseminated and bedding-parallel sulphides from Luiswishi (after Lerouge et al. 2005) and of anhydrite in the Zambian Copperbelt (after Dechow and Jensen 1965) are shown for comparison

Discussion

A model is proposed here that explains the origin of the pseudomorphs after anhydrite, taking into account several observations: (1) the replacement of anhydrite by dolomite and the subsequent replacement of dolomite by Cu–Co sulphides and quartz, preferentially along the rim of the nodule; (2) the typical association of the sulphides with authigenic quartz; (3) the dissolution of detrital quartz in the siltstones; (4) the negative $\delta^{34}S$ values of the metal sulphides in the pseudomorphs; (5) the depletion in the oxygen and carbon isotopic composition of the dolomites in pseudomorphs compared to marine Neoproterozoic dolomites; (6) the high salinity of the mineralising fluid; (7) the variation in the proportion of the minerals (dolomite, authigenic quartz and Cu–Co sulphides) in the pseudomorphs; and (8) the abundance of carrolite in the pseudomorphs.

The sulphur isotopic composition of the sulphides between −10.3 and +3.1‰ V-CDT is within the range reported for disseminated and bedding-parallel sulphides from the lower and upper orebodies at Luiswishi (Fig. 6, Lerouge et al. 2005) and for diagenetic pyrite in black shales in the Zambian Copperbelt (McGowan et al. 2003, 2006). The $\delta^{34}S$ values of the Lower Roan anhydrite nodules in the Copperbelt are between +12 and +22‰ V-CDT (Fig. 7, Dechow and Jensen 1965). An average $\delta^{34}S$ value of +17.5‰ V-CDT is suggested for Late Neoproterozoic seawater (Claypool et al. 1980). Taking this into account, calculated ΔSO_4–H_2S values for the copper–cobalt sulphides in the evaporite pseudomorphs fall between +14.4 and +27.8‰, consistent with fractionation values typical of bacterial sulphate reduction (Ohmoto 1986; Machel et al. 1995). Therefore, the replacement of anhydrite by dolomite is interpreted to be mainly related to bacterial sulphate reduction (BSR) occurring in the anhy-

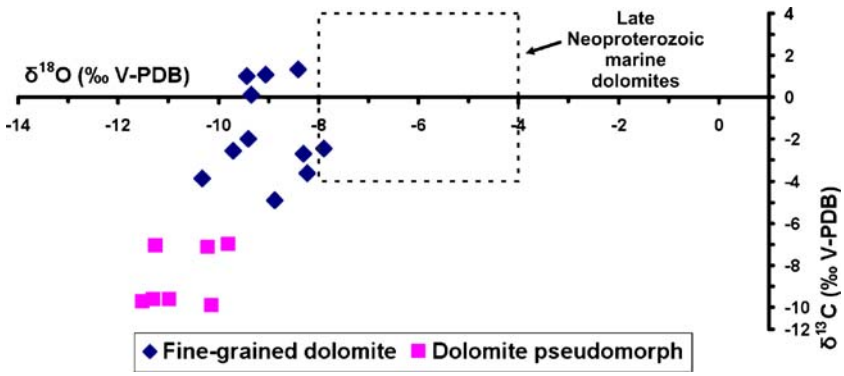

Fig. 8 Carbon and oxygen isotope composition of fine-grained dolomite of the Mines Subgroup and of hypidiotopic dolomite pseudomorphs after anhydrite. Also shown is the isotopic composition of Neoproterozoic marine dolomites (after Veizer and Hoefs 1976)

Table 1 Rb–Sr isotopic and concentration data for dolomite samples from evaporite pseudomorphs

Sample	$^{87}Rb/^{86}Sr$	2σ	$^{87}Sr/^{86}Sr$	2σ	Sr (ppm)	2σ	Rb (ppm)	2σ
KA07HA04	0.0177	0.0003	0.71021	0.00002	7.13	0.05	0.0437	0.0005
KA05VD011	n.d.	n.d	0.71025	0.00002	31.18	0.22	n.d.	n.d
KA05VD012	0.0043	0.0001	0.71120	0.00018	16.11	0.11	0.0240	0.0003
KA07HA18	n.d.	n.d	0.71309	0.00002	19.76	0.11	n.d.	n.d
KA07HA20	0.0130	0.0002	0.73408	0.00002	18.51	0.08	0.0832	0.0009
KA07HA21	0.0933	0.0010	0.73576	0.00002	22.33	0.10	0.7182	0.0073
KA07HA22	0.0260	0.0004	0.71493	0.00001	14.75	0.12	0.1324	0.0015
KA07HA24	0.0561	0.0006	0.71038	0.00003	41.87	0.32	0.8110	0.0077
KA07HA28	0.0928	0.0008	0.71332	0.00002	33.18	0.16	1.0640	0.0091
KA05VD062	n.d.	n.d	0.71024	0.00002	29.32	0.23	n.d.	n.d
KA05VD065	n.d.	n.d	0.71223	0.00003	40.61	0.26	n.d.	n.d
KA05VD066	n.d.	n.d	0.71012	0.00001	41.08	0.22	n.d.	n.d

n.d. not determined

drite nodules. However, this model does not change even when there is a contribution of sulphide from thermochemical sulphate reduction by hot mineralising fluids (Hoy and Ohmoto 1989) since the sequence of reactions remains the same.

The net mass balance reaction for the sulphate reduction can be described by the following general equation (Machel 1987):

$$\text{organic matter} + SO_4^{2-} \Rightarrow \text{altered organic matter} + H_2S\,(HS^-) + HCO_3^-(CO_2) + H_2O \quad (1)$$

The reductant could have been provided by organic matter surrounding the nodules and disseminated in the siltstones (Cailteux 1994) or by cyanobacterial mats in the laminated carbonates (Bartholomé et al. 1972). Calcite often replaces calcium sulphate (Machel 2001), as observed

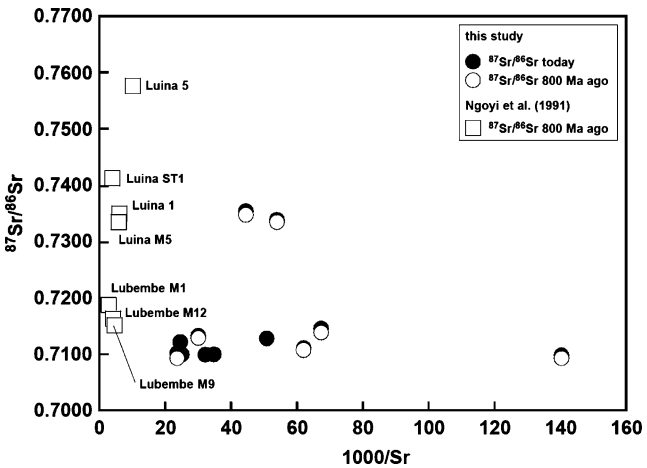

Fig. 9 Comparative $^{87}Sr/^{86}Sr$ vs. 1,000/Sr mixing diagram for dolomite samples from evaporite pseudomorphs (this study) and granite samples from the basement in the Luina area (Katanga, DRC; Ngoyi et al. 1991)

in the widespread occurrence of calcite cements in environments affected by BSR (Sassen et al. 1988). In addition to calcite, dolomite may form when the host carbonate rock is a dolostone (Machel et al. 1995; Machel 2001). In the Katanga Copperbelt, the earliest mineral that replaced anhydrite in the dolomitic siltstone and dolomite was indeed dolomite:

$$Ca^{2+} + Mg^{2+} + 2CO_2 + H_2O \Leftrightarrow CaMg(CO_3)_2 + 4H^+ \quad (2)$$

An important observation is the close association of sulphides with large amounts of authigenic quartz in the pseudomorphs. Precipitation of large amounts of quartz is only possible if sufficient volumes of a silica-rich fluid migrated through the siltstones and dolomites. Si-rich fluids are characterised by an elevated pH (Hesse 1989). The significant amount of copper–cobalt sulphides in the pseudomorphs implies an open to semi-open system for the mineralising fluids, allowing efficient mass transfer of the metals (Garven 1995).

The saline, metal-bearing fluids migrated through the sediments and, in the vicinity of the pseudomorphs, reacted with H_2S formed during BSR, resulting in the precipitation of sulphides:

$$Me^{2+} + H_2S \Rightarrow MeS + 2H^+ \quad (3)$$

Precipitation first occurred around the rim of the pseudomorphs and continued towards the core. Sometimes the core still consists of anhydrite. During precipitation of sulphides, hydrogen ions are released which are interpreted to have caused a decrease in pH and precipitation of authigenic quartz (Williams and Crerar 1985; Hesse 1988). Brown (2005) already suggested that the mineralising fluid in sediment-hosted stratiform copper deposits could be

buffered by silicate constituents of the basin fill. The solubility of quartz increases significantly with pH (Williams and Crerar 1985). A pH decrease may also cause the dissolution of earlier formed dolomite in the pseudomorphs and of the more fine-grained dolomite in the host rock. Due to the fine-grained nature of the host rock dolomite, this could not be observed. However, there are abundant dissolution cavities in the dolomite filled with authigenic quartz and Cu–Co sulphides. The dissolved dolomite forms an additional source for the dolomitic cement that later replaced the anhydrite in the more central parts of the anhydrite nodule.

A comparable mineralising model has been proposed for the sediment-hosted Zn–Pb deposit at Navan, Ireland (Anderson et al. 1998; Fallick et al. 2001). Here, it was suggested that sulphide was derived from bacterial reduction of sulphate, whereas metals were transported to the site of ore deposition by a hot fluid originating from the basement.

Since BSR occurs at temperatures from 0 up to about 80°C (Machel 2001), this reaction did not occur during the infiltration of the hot mineralising fluid, with temperatures up to 190°C (Dewaele et al. 2006). Although, in general, authigenic quartz and sulphides replace dolomite, different successive phases may be recognised and the proportions of the three minerals may vary significantly within the nodules between different layers. However, within one layer, the mineralogical composition of the pseudomorphs is rather constant. The replacement of anhydrite nodules from the rim towards the centre is typical of these pseudomorphs and implies that transport towards the centre remains possible (Ulmer-Scholle et al. 1993; Alonso-Zara et al. 2002).

The process responsible for the silica concentration in solution remains unclear. Dissolution of detrital quartz has been observed in the dolomitic siltstones, resulting in the absence of detrital quartz in layers characterised by clusters of authigenic quartz and by the formation of massive authigenic quartz with enclosed, randomly oriented phyllosilicates. This dissolved silica may have formed the source of the authigenic quartz; however, other sources cannot be ruled out.

Characteristic is the high amount of carrolite in the rocks which are rich in pseudomorphs after anhydrite. This can be explained by the high sulphur activity in the host rock due to BSR. Craig et al. (1979) demonstrated that the type of mineral species that precipitates in the Cu–Co–S system mainly depends on temperature and sulphur activity. Carrolite especially forms at very high sulphur activities, in agreement with the large amounts of sulphur available in the anhydrite nodules.

The source of high-salinity base metal mineralising brines has been investigated in numerous studies of sediment-hosted ore deposits worldwide (Viets et al. 1996; Banks et al. 2002; Grandia et al. 2003; Heijlen et al. 2003). Mostly, the brines were generated by evaporation of seawater in a restricted environment (see Muchez et al. 2005 for a review of Zn–Pb mineralising brines in Europe). These high-salinity fluids migrated in the subsurface and often into the underlying basement (Everett et al. 1999; Gleeson and Yardley 2003). In the Copperbelt, evaporitic conditions existed during the sedimentation of the R.A.T., Mines and Dipeta Subgroups, as evidenced by the abundance of pseudomorphs after anhydrite and early diagenetic magnesite (Cailteux et al. 2005).

The carbon and oxygen isotopic composition of the host rock dolomite partly falls within the range of Neoproterozoic marine dolomite (Veizer and Hoefs 1976; Lindsay et al. 2005). Such a marine origin is in agreement with models proposed by Bartholomé et al. (1972) and Cailteux (1973, 1994). Bartholomé et al. (1972) envisaged dolomitisation by reflux of hypersaline fluids that formed in the lagoonal sedimentary environment. Dolomite precipitation in an intertidal to supratidal environment was proposed for the fine-grained dolomites by Cailteux (1973, 1994). Dolomites that form in a marine environment during sedimentation and early diagenesis are often partly or completely recrystallised (Land 1980; Smith and Dorobek 1993; Nielsen et al. 1994). In these studies, the carbon and oxygen isotopic values of dolomites that are below the marine isotope values have been explained by recrystallisation, possibly under the influence of the mineralising fluids that migrated through the rocks. The isotopic composition of dolomite replacing the anhydrite nodules is also lower than the isotopic composition of marine dolomite. The lowest $\delta^{18}O$ value of −11.50‰ V-PDB can be explained by dolomite precipitation from seawater at a maximum temperature between 55 and 70°C (cf. O'Neil et al. 1969), and thus within the temperature range of bacterial sulphate reduction. Dolomite with higher $\delta^{18}O$ values precipitated at lower temperatures. The low $\delta^{13}C$ values are the result of preferential incorporation of ^{12}C, generated during the oxidation of organic matter (Irwin et al. 1977). This oxidation can be related to reaction (1).

Several carbon and isotopic studies on dolomite have been carried out in the Zambian part of the Copperbelt (Sweeney et al. 1986; Selley et al. 2005; McGowan et al. 2006). Sweeney et al. (1986) studied the isotopic composition of dolomitic lenses that varied between $\delta^{13}C=-8.77$ and −20.52‰ V-PDB and $\delta^{18}O=-14.45$ and −19.39‰ V-PDB. They suggested the carbon isotopic values to be indicative of an organic carbon source and that the organic matter was oxidised during early diagenetic dolomitisation of the lenses. The $\delta^{18}O$ data were interpreted to reflect the influence of both fresh and marine waters; however, no arguments were given that exclude other interpretations such as an influence of elevated temperatures on the

precipitation of this dolomite. Possibly, the precipitation of the dolomite lenses occurred at high temperature such as has been recognised in type 2 dolomite at Luiswishi. Its carbon and oxygen isotopic composition is similar to that of late diagenetic to syn-orogenic dolomite veins at Nkana ($\delta^{13}C$=−11.97 to −19.5‰ V-PDB and $\delta^{18}O$=−14.5 to −18.6‰ V-PDB, Brems 2007). A similar range in oxygen isotope values has been reported for dolomite from the alteration zone within the upper orebody and a shear zone at the Nchanga deposit ($\delta^{18}O$=−13.6 to −18.6‰ V-PDB, McGowan et al. 2006). The $\delta^{13}C$ values of these dolomites are, however, less negative and between −2.9 and −8.3‰ V-PDB. In the extensive study of Selley et al. (2005), 369 carbonate samples (whole rock, veins and evaporite nodules) were analysed, confirming a trend recognised by earlier workers (Annels 1989; Sweeney and Binda 1989) from values typical of Neoproterozoic marine carbonates ($\delta^{13}C$=−4.0 to +4.0‰ V-PDB and $\delta^{18}O$=−8 to −4 ‰ V-PDB; Veizer and Hoefs 1976; Lindsay et al. 2005) in the unaltered sedimentary carbonates to isotopically light values ($\delta^{13}C$=−4.0 to −26‰ V-PDB and $\delta^{18}O$=−8 to −25‰ V-PDB). Carbon and oxygen isotope data are consistent with the introduction of an organic carbon component at higher temperature (Selley et al. 2005; McGowan et al. 2006). Existing data and our study suggest that organic carbon played an important role in the precipitation of dolomite, but there is no criterion to distinguish early from late oxidation reactions. The wide range of measured oxygen isotope values could be due to a variation in the precipitation temperature of the dolomite, variation in the isotopic composition of the dolomitising fluid, variable interaction of the ambient fluid with the host rock or a combination of these processes. The oxygen isotope data of dolomite in the type 1 nodules, layers and bands at Kamoto only indicate that if dolomite precipitation occurred from seawater, the calculated temperature of the dolomitising fluid was between 55 and 70°C using the fractionation factors published by O'Neil et al. (1969), and thus is within the range of bacterial sulphate reduction. Dolomite with a $\delta^{18}O$ of −20‰ V-PDB precipitated at a temperature of ~130°C from a fluid with seawater oxygen isotope signature. This temperature is above the range of bacterial sulphate reduction, but at the onset of thermochemical sulphate reduction (Machel 2001).

Radiogenic Sr isotopic compositions of some dolomite samples unrelated to significant in situ decay of ^{87}Rb indicate that the strontium not only was derived from the Neoproterozoic carbonate host rock but also interacted with siliciclastic rocks. Sr isotope data on Neoproterozoic rocks and the basement in the study area are scarce and a detailed comparison with the different rock types is not yet possible. Ngoyi et al. (1991) presented some Rb–Sr data for whole rocks from the granitic basement exposed at Luina (Katanga, DRC). The $^{87}Sr/^{86}Sr$ ratios of these samples vary between 0.777 and 0.895 (n=6), with one value at 1.408. The $^{87}Sr/^{86}Sr$ vs. 1,000/Sr mixing diagram (Fig. 9) shows a good correspondence in Sr isotopic compositions recalculated to 800 Ma between the granites from the Luina area and the dolomite samples from Kamoto, indicating that the granitic basement could have been a viable source for Sr. An age of 800 Ma is used based on Re–Os dating of chalcopyrite in the hangingwall at the Konkola deposit, near the Luina dome, at 816±62 Ma (in Selley et al. 2005). This is the oldest age published for the Cu–Co ore deposits in the Copperbelt and in agreement with a diagenetic origin of the mineralisations (Muchez et al. 2007).

However, the arkoses at Nchanga are also radiogenic with values around 0.73 (Steve Roberts, personal communication). At this stage, we can only conclude that the mineralising fluid interacted with siliciclastic rocks in the Roan Group and/or the underlying basement.

Conclusions

Two types of pseudomorphs of anhydrite nodules and lenses are distinguished in the stratiform Cu–Co ore deposits hosted by the Mines Subgroup of the Roan Group. In type 1, dolomite precipitated first and was replaced by Cu–Co sulphides and authigenic quartz. Authigenic quartz and sulphides in type 2 precipitated prior to dolomite and the crystals are coarse-grained and freely growing.

Based on the negative $\delta^{34}S$ values of −10.3 to +3.1‰ V-CDT of the metal sulphides in the type 1 evaporite pseudomorphs, the replacement of the type 1 nodules and lenses is interpreted to be related to bacterial reduction of sulphate derived from primary anhydrite. Generation of CO_2 during this reaction caused the precipitation of dolomite. When the mineralising fluid reached the BSR reaction site, the H_2S reacted with the metals Cu, Co and Fe to form sulphides such as carrolite, bornite, chalcopyrite and chalcocite. During sulphide precipitation, hydrogen ions were released, causing a decrease in pH and precipitation of authigenic quartz.

The mineralising fluid had a high salinity (8 to 18 eq. wt. % NaCl) and is thought to represent evaporated seawater of Roan age that migrated through the deeper subsurface, thereby causing dolomitisation of the host rocks and mobilising Sr from siliciclastic rocks significantly more radiogenic than that of Neoproterozoic seawater. The distinct negative carbon isotopic composition of dolomite in the pseudomorphs ($\delta^{13}C$=−7.10 and −9.93‰ V-PDB) is due to the incorporation of light carbon generated by the oxidation of organic matter.

Acknowledgements We are grateful to Steve Roberts and Robert Moritz for their constructive reviews and thoughtful suggestions and to Bernd Lehmann for editing this paper. We would like to thank E. Pirard (Université de Liège) for the permission to study borehole 120 from Kamoto. We are grateful to Dr. M. Joachimski of the University of Erlangen for the stable isotope analysis. We thank Herman Nijs for the careful preparation of the numerous thin and polished sections.

This research is financially supported by the research grants G.0585.06 and G.0414.08 of the FWO-Vlaanderen.

References

Allsopp HL, Ferguson J (1970) Measurements relating to the genesis of the Tsumeb pipe, South West Africa. Earth Planet Sci Lett 9:448–445

Alonso-Zara AM, Sánchez-Moya Y, Sopeña A, Delgado A (2002) Silicification and dolomitisation of anhydrite nodules in argillaceous terrestrial deposits: an example of meteoric-dominated diagenesis from the Triassic of Central Spain. Sedimentology 49:303–317

Anderson IK, Ashton JH, Boyce AJ, Fallick AE, Russell MJ (1998) Ore depositional processes in the Navan Zn–Pb deposit, Ireland. Econ Geol 93:535–563

Annels AE (1974) Some aspects of the stratiform ore deposits of the Zambian Copperbelt and their genetic significance. Centenaire Soc Geol Belg 102:431–449

Annels AE (1989) Ore genesis in the Zambian Copperbelt with particular reference to the northern sector of the Chambishi Basin. In: Boyle RW, Brown AC, Jefferson CW, Jowett EC, Kirkham RV (eds) Sediment-hosted stratiform copper deposits. Geological Association of Canada, Special Paper 36:427–452

Armstrong RA, Master S, Robb LJ (2005) Geochronology of the Nchanga Granite, and constraints on the maximum age of the Katanga Supergroup, Zambian Copperbelt. J Afr Earth Sci 42:32–40

Banks DA, Boyce AJ, Samson IM (2002) Constraints on the origins of fluids forming Irish Zn–Pb–Ba deposits: evidence from the composition of fluid inclusions. Econ Geol 97:471–480

Bartholomé P (1974) On the diagenetic formation of ores in sedimentary beds, with special reference to Kamoto, Shaba, Zaïre. In: Bartholomé P (ed) Gisements stratiformes et provinces cuprifère. Centenaire de la Sociéte Géologique de Belgique, Liège, pp 203–214

Bartholomé P, Evrard P, Katekesha F, Lopez-Ruiz J, Ngongo M (1972) Diagenetic ore-forming processes at Kamoto, Katanga, Republic of the Congo. In: Amstutz GC, Bernard AJ (eds) Ores in sediments. Springer, Berlin, pp 21–41

Batumike MJ, Cailteux JLH, Kampunzu AB (2007) Lithostratigraphy, basin development, base metal deposits, and regional correlations of the Neoproterozoic Nguba and Kundelungu rock succession, central African Copperbelt. Gondwana Res 11:432–447

Birck L (1986) Precision K–Rb–Sr isotopic analysis: application to Rb–Sr chronology. Chem Geol 56:73–83

Brems D (2007) Petrografische, mineralogische en geochemische studie van de Nkana Cu–Co afzetting, Zambia. Unpublished licentiate thesis, K.U.Leuven

Brown AC (2005) Refinements for footwall red-bed diagenesis in the sediment-hosted stratiform copper deposits model. Econ Geol 100:765–771

Brown AC, Chartrand FM (1983) Stratiform copper deposits and interactions with co-existing atmospheres, hydrospheres, biospheres and lithospheres. Precambrian Res 20:533–542

Cailteux J (1973) Minerais cuprifères et roches encaissantes à Musoshi, province du Shaba, République du Zaïre. Ann Soc Geol Belg 96:495–521

Cailteux J (1978a) Particularités stratigraphiques et pétrographiques du faisceau inférieur du Groupe des mines au centre de l'arc cuprifère shabien. Ann Soc Geol Belg 100:55–71

Cailteux J (1978b) La succession stratigraphique du C.M.N. (ou R 2.3) au centre de la sous province cuprifère shabienne. Ann Soc Geol Belg 100:73–85

Cailteux J (1994) Lithostratigraphy of the Neoproterozoic Shaba-type (Zaire) Roan Supergroup and metallogenesis of associated stratiform mineralization. J Afr Earth Sci 19:279–301

Cailteux J (1997) Minéralisation à U–Pb–Se–Mo–Ni dans le gisements stratiforme cupro-cobaltifère de Kambove-Ouest (Shaba, Rép. Zaïre). In: Charlet J-M (ed) International Cornet Symposium 'Strata-bound Copper Deposits and Associated Mineralizations'. Faculté Polytechnique de Mons and Royal Academy of Overseas Sciences, Liège, pp 245–286

Cailteux J, Kampunzu AB (2003) Third workshop of IGCP 450: Proterozoic sediment-hosted base metal deposits of Western Gondwana. Episodes 23:209–213

Cailteux J, Binda PL, Katekesha WM, Kampunzu AB, Intiomale MM, Kapenda D, Kaunda C, Ngongo K, Tshiauka T, Wendorff M (1994) Lithostratigraphical correlation of the Neoproterozoic Roan Supergroup from Shaba (Zaire) and Zambia, in the central African copper–cobalt metallogenic province. In: Kampunzu AB, Lubala RT (eds) Neoproterozoic belts of Zambia, Zaire and Namibia. Journal of African Earth Sciences 19:265–278

Cailteux JLH, Kaputo AK, Kampunzu AB (2003) Structure, lithostratigraphy and Cu–Co mineralization of the Mines Subgroup at Luiswishi, central Africa Copperbelt. In: Cailteux J (ed) Proterozoic sediment-hosted base metal deposits of Western Gondwana, Lubumbashi, pp 103–107

Cailteux JLH, Kampunzu AB, Lerouge C, Kaputo AK, Milesi JP (2005) Genesis of sediment-hosted stratiform copper–cobalt deposits, central African Copperbelt. J Afr Earth Sci 42:134–158

Cailteux JLH, Kampunzu AB, Lerouge C (2007) The Neoproterozoic Mwashya–Kansuki sedimentary rock succession in the central African Copperbelt, its Cu–Co mineralization, and regional correlations. Gondwana Res 11:414–431

Claypool GE, Holser WT, Kaplan IR, Sakai H, Zak I (1980) The age curves of sulphur and oxygen isotopes in marine sulphate and their mutual interpretation. Chem Geol 28:199–260

Craig JR, Vaughan DJ, Higgins JB (1979) Phase relations in the Cu–Co–S system and mineral associations of the carrolite ($CuCo_2S_4$)–linnaeite (Co_3S_4) series. Econ Geol 74:657–671

Daly MC, Chakroborty SK, Kasolo P, Musiwa M, Mumba P, Naidu B, Namateba C, Ngambi O, Coward MP (1984) The Lufilian arc and Irumide belt of Zambia: results of a geotraverse across their intersection. J Afr Earth Sci 2:311–316

Dechow E, Jensen ML (1965) Sulphur isotopes of some Central African sulphide deposits. Econ Geol 60:894–941

Deniel C, Pin C (2001) Single-stage method for the simultaneous isolation of lead and strontium from silicate samples for isotopic measurements. Anal Chim Acta 426:95–103

Dewaele S, Muchez Ph, Vets J, Fernandez-Alonzo M, Tack L (2006) Multiphase origin of the Cu–Co ore deposits in the western part of the Lufilian fold-and-thrust belt, Katanga (Democratic Republic of Congo). J Afr Earth Sci 46:455–469

El Desouky HA, Muchez Ph, Dewaele S, Boutwood A, Tyler R (2007a) The stratiform copper mineralization of the Lufukwe anticline, Lufilian foreland, Democratic Republic Congo. Geol Belg 10:148–151

El Desouky H, Haest M, Muchez Ph, Dewaele S, Cailteux J, Heijlen W (2007b) Fluid evolution in the Katanga Copperbelt, DRC. In:

Andrew CJ et al (ed) Digging deeper. Proceedings of the 9th SGA meeting, Dublin 2007 (Ireland). Irish Association for Economic Geology, Dublin, pp 213–216

Everett CE, Wilkinson JJ, Rye DM (1999) Fracture-controlled fluid flow in the Lower Palaeozoic basement rocks of Ireland: implications for the genesis of Irish-type Zn–Pb deposits. In: McCaffrey KJW, Lonergan L, Wilkinson JJ (eds) Fractures, fluid flow and mineralization special publication 155. Geological Society, London, pp 247–276

Fallick A, McConville P, Boyce AJ, Burgess R, Kelley SP (1992) Laser microprobe stable isotope measurements on geological materials: some experimental considerations (with special reference to $d^{34}S$ in sulphides). Chem Geol 101:53–61

Fallick AE, Ashton JH, Boyce AJ, Ellam RM, Russell MJ (2001) Bacteria were responsible for the magnitude of the world-class hydrothermal base metal sulphide orebody at Navan, Ireland. Econ Geol 96:885–890

François A (1974) Stratigraphie, tectonique et minéralisation dans l'arc cuprifère du Shaba. Centenaire de la Société Géologiques de Belgique. Gisements stratiformes et provinces cuprifères. Liège, 79–101

Friedman GM (1965) Terminology of crystallization textures in sedimentary rocks. J Sediment Petrol 35:643–655

Garven G (1995) Continental-scale groundwater flow and geological processes. Annu Rev Earth Planet Sci 23:89–117

Gleeson SA, Yardley BWD (2003) Surface-derived fluids in basement rocks: inferences from palaeo-hydrothermal systems. J Geochem Explor 78–79:61–65

Grandia F, Cardellach E, Canals A, Banks DA (2003) Geochemistry of the fluids related to epigenetic carbonate-hosted Zn–Pb deposits in the Maestrat Basin, eastern Spain: fluid inclusion and isotope (Cl, C, O, S, Sr) evidence. Econ Geol 98:933–954

Heijlen W, Muchez Ph, Banks DA, Schneider J, Kucha A, Keppens E (2003) Carbonate-hosted Zn–Pb deposits in Upper Silesia, Poland: origin and evolution of mineralizing fluids and constraints on genetic models. Econ Geol 98:911–932

Hesse R (1988) Origin of chert: diagenesis of biogenic siliceous sediments. Geosci Canada 15:171–192

Hesse R (1989) Silica diagenesis: origin of inorganic and replacement cherts. Earth-Sci Rev 26:253–284

Hitzman M, Kirkham R, Broughton D, Thorson J, Selley D (2005) The sediment-hosted stratiform copper ore system. Econ Geol 100th Anniversary Volume. Society of Economic Geology, Tulsa, pp 609–642

Hoy LD, Ohmoto H (1989) Constraints for the genesis of redbed-associated stratiform Cu deposits from sulphur and carbon mass-balance relations. In: Boyle RW, Brown AC, Jefferson CW, Jowett EC, Kirkham RV (eds) Sediment-hosted Stratiform Copper Deposits. Geological Association of Canada, Special Paper 36:135–149

Irwin H, Curtis C, Coleman M (1977) Isotopic evidence for source of diagenetic carbonates formed during burial of organic-rich sediments. Nature 269:209–213

Jacobsen SB, Kaufman AJ (1999) The Sr, C and O isotopic evolution of Neoproterozoic seawater. Chem Geol 161:37–57

Kampunzu AB, Cailteux JLH (1999) Tectonic evolution of the Lufilian Arc (Central Africa Copper Belt) during Neoproterozoic pan African orogenesis. Gondwana Res 2:401–421

Kampunzu AB, Tembo F, Mathies G, Kapenda D, Huntsman-Mapila P (2000) Geochemistry and tectonic setting of mafic igneous units in the Neoproterozoic Katangan basin, central Africa: implications for Rodinia break up. Gondwana Res 3:125–153

Kelley SP, Fallick AE (1990) A high precision spatially resolved analysis of $d^{34}S$ in sulphides using a laser extraction technique. Geochim Cosmochim Acta 54:883–888

Key RM, Liyungu AK, Njamu FM, Somwe V, Banda J, Mosley PN, Armstrong RA (2001) The western arm of the Lufilian Arc in NW Zambia and its potential for copper mineralization. J Afr Earth Sci 33:503–528

Land LS (1980) The isotopic and trace element geochemistry of dolomite: the state of the art. In: Zenger DH, Dunham JB, Ethington RL (eds) Concepts and models of dolomitisation. The Society of Economic Paleontologists and Mineralogists Special Publication 28:87–110

Lefebvre J-J (1978) Le Groupe de Mwashya, mégacyclthème terminal du Roan (Shaba, Zaïre Sudoriental). I—Approche lithostratigraphique et étude de l'environnement sédimentaire. Ann Soc Geol Belg 101:209–225

Lefebvre J-J (1989) Depositional environment of copper–cobalt mineralization in the Katangan sediments of southeast Shaba, Zaïre. In: Boyle RW, Brown AC, Jefferson CW, Jowett EC, Kirkham RV (eds) Sediment-hosted stratiform copper deposits. Geological Association of Canada, Special Paper 36:401–426

Lerouge C, Cailteux J, Kampunzu AB, Milesi JP, Fléhoc C (2005) Sulphur isotope constraints on formation conditions of the Luiswishi ore deposit, Democratic Republic of Congo (DRC). J Afr Earth Sci 42:173–182

Lindsay JF, Kruse PD, Green OR, Hawkins E, Brasier MD, Cartlidge J, Corfield RM (2005) The Neoproterozoic–Cambrian record in Australia: a stable isotope study. Precambrian Res 143:113–133

Machel HG (1987) Some aspects of diagenetic sulphate–hydrocarbon redox-reactions. In: Marshall JD (ed) Diagenesis of sedimentary sequences. Geological Society Special Publication 36:15–28

Machel HG (2001) Bacterial and thermochemical sulfate reduction in diagenetic settings—old and new insights. Sediment Geol 140:143–175

Machel HG, Krouse HR, Sassen R (1995) Products and distinguishing criteria of bacterial and thermochemical sulfate reduction. Appl Geochem 10:373–389

Machel HG, Foght J (2000) Products and depth limits of microbial activity in petroliferous subsurface settings. In: Riding RE, Awramik SM (eds) Microbial sediments. Springer, Berlin, pp 105–120

Master S, Rainaud C, Armstrong RA, Phillips D, Robb LJ (2005) Provenance ages of the Neoproterozoic Katanga Supergroup (Central African Copperbelt), with implications for basin evolution. J Afr Earth Sci 42:41–60

McGowan RR, Roberts S, Foster RP, Boyce AJ, Coller D (2003) Origin of the copper–cobalt deposits of the Zambian Copperbelt: an epigenetic view from Nchanga. Geology 31:497–500

McGowan RR, Roberts S, Boyce AJ (2006) Origin of the Nchanga copper–cobalt deposits of the Zambian Copperbelt. Miner Depos 40:617–638

Muchez Ph, Heijlen W, Banks D, Blundell D, Boni M, Grandia F (2005) Extensional tectonics and the timing and formation of basin-hosted deposits in Europe. Ore Geol Rev 27:241–267

Muchez Ph, Brems D, El Desouky H, Haest M, Vanderhaeghen P, Dewaele S, Heijlen W, Mukumba W (2007) Base metal ore deposit evolution and geodynamics in the Central African Coppernelt. In: Andrew CJ et al (ed) Digging deeper. Proceedings of the 9th SGA meeting, Dublin 2007 (Ireland). Irish Association for Economic Geology, Dublin, pp 209–212

Ngoyi K, Liégeois J-P, Demaiffe D, Dumont P (1991) Age tardi-ubendien (Protérozoïque inférieur) des dômes granitiques de l'arc cuprifère zaïro-zambien. C R Acad Sci Paris 313:83–89

Nielsen P, Swennen R, Keppens E (1994) Multiple-step recrystallization within massive ancient dolomite units: an example from the Dinantian of Belgium. Sedimentology 41:567–584

Ohmoto H (1986) Stable isotope geochemistry of ore deposits. In: Valley JW, Taylo HP, O'Neil JR (eds) Stable isotopes in high temperature geological processes. Reviews in Mineralogy 16, Mineralogical Society of America, pp 491–559

Okitaudji LR (1992) Interprétation sédimentologique du Roan (Précambrien supérieur) du Shaba (Zaïre) et place des minéralisations cupro-cobaltifères. J Afr Earth Sci 14:371–386

O'Neil JR, Clayton RN, Mayeda TK (1969) Oxygen isotope fractionation in divalent metal carbonates. J Chem Phys 51:5547–5558

Sassen R, Chinn EW, McCabe C (1988) Recent hydrocarbon alteration, sulphate reduction and formation of elemental sulfur and metal sulfides in salt dome cap rock. Chem Geol 74:57–66

Selley D, Broughton D, Scott R, Hitzman M, Bull S, Large R, McGoldrick P, Croaker M, Pollington N, Barra F (2005) A new look at the geology of the Zambian Copperbelt. Economic Geology 100th Anniversary Volume. Society of Economic Geology, Tulsa, pp 965–1000

Smith TM, Dorobek SL (1993) Alteration of early-formed dolomite during shallow to deep burial: Mississippian Mission Canyon Formation, central to southwestern Montana. Geol Soc Am Bull 105:1389–1399

Sweeney MA, Binda PL (1989) The role of diagenesis in the formation of the Konkola Cu–Co orebody of the Zambian Copperbelt. In: Boyle RW, Brown AC, Jefferson CW, Jowett EC, Kirkham RV (eds) Sediment-hosted stratiform copper deposits. Geological Association of Canada, Special Paper, 36, pp 499–518

Sweeney MA, Turner P, Vaughan DJ (1986) Stable isotope and geochemical studies of the role of early diagenesis in ore formation, Konkola basin, Zambian Copperbelt. Econ Geol 91:1838–1852

Ulmer-Scholle DS, Scholle PA, Brady PV (1993) Silicification of evaporates in Permian (Guadalupian) back-reef carbonates of the Delaware Basin, West Texas and New Mexico. J Sediment Petrol 63:955–965

Veizer J, Hoefs J (1976) The nature of $^{18}O/^{16}O$ and $^{13}C/^{12}C$ secular trends in sedimentary carbonate rocks. Geochim Cosmochim Acta 40:1387–1395

Viets DL, Hofstra AF, Emsbo P (1996) Solute compositions of fluid inclusions in sphalerite from North America and European Mississippi Valley-type ore deposits: ore fluids derived from evaporated seawater. In: Sangster DF (ed) Carbonate-hosted lead–zinc deposits. Society of Economic Geologists Special Publication 4, pp 465–482

Wachter E, Hayes JM (1985) Exchange of oxygen isotopes in carbon-dioxide–phosphoric acid systems. Chem Geol 52:365–374

Williams LA, Crerar DA (1985) Silica diagenesis. II. General mechanisms. J Sediment Petrol 55:312–321